Applied Physics Letters

Ultrafast magnetism: The magneto-optical Kerr effect and conduction electrons

Cite as: Appl. Phys. Lett. **116**, 112404 (2020); https://doi.org/10.1063/1.5143115
Submitted: 19 December 2019 . Accepted: 11 March 2020 . Published Online: 20 March 2020

R. Gort, K. Bühlmann, G. Saerens, S. Däster, A. Vaterlaus, and Y. Acremann

Applied Physics Letters ARTICLE scitation.org/journal/apl

Ultrafast magnetism: The magneto-optical Kerr effect and conduction electrons

Cite as: Appl. Phys. Lett. **116**, 112404 (2020); doi: 10.1063/1.5143115
Submitted: 19 December 2019 · Accepted: 11 March 2020 ·
Published Online: 20 March 2020

R. Gort,[1,2,a] K. Bühlmann,[1] G. Saerens,[1] S. Däster,[1] A. Vaterlaus,[1] and Y. Acremann[1,b]

AFFILIATIONS

[1]Laboratory for Solid State Physics, ETH Zurich, 8093 Zurich, Switzerland
[2]European XFEL GmbH, Holzkoppel 4, 22869 Schenefeld, Germany

[a]Electronic mail: rafael.gort@xfel.eu
[b]Author to whom correspondence should be addressed: acremann@solid.phys.ethz.ch

ABSTRACT

Most experiments on ultrafast magnetodynamics have been conducted using the magneto-optical Kerr effect. Here, we compare the Kerr effect's magnetic sensitivity to the spin dynamics measured by photoemission. The magnetization dynamics on an Fe/W(110) thin film are probed by spin-resolved photoemission spectroscopy and the Kerr effect. The results reveal similarities between the spin dynamics at low binding energy and the response probed by the Kerr effect. Therefore, the Kerr effect probes states relevant for spin transport and spin flips but may not be sensitive to the entire magnetic moment in femtosecond spin dynamics experiments.

The investigation of non-equilibrium states of magnetization has become more relevant for applications of magnetism in magnetic storage and memory devices. A prominent example is the use of magnetic toggle switching in memory devices.[1] Another example is the use of heating pulses in a hard disk drive to temporarily reduce the magnetic field required for writing.[2]

If we slowly heat a ferromagnetic material to Curie temperature, we expect to see the reduction and subsequently the loss of magnetization. This demagnetization will be apparent for all known detection schemes of magnetization: We can use the magneto-optic Kerr effect (MOKE), spin polarized photoelectron spectroscopy (SPES), and x-ray circular magnetic dichroism (XMCD) to detect a quantity that is proportional to magnetization. With the development of femtosecond lasers, it has become possible to drive different sub-systems of the ferromagnet out of equilibrium: the electron gas, lattice, and spin system can be at different temperatures at the same time. The discovery of femtosecond demagnetization[3] led to a debate if the application of the magneto-optical Kerr effect is valid to detect the magnetization in a sample, which is far from equilibrium: The magnetization is probed indirectly through the spin–orbit coupling, which may be affected by the pump pulse.

These concerns were raised in early years[4–11] and have been addressed on an experimental[8] as well as on a theoretical basis.[11] However, since a large variety of optical transitions contribute to the measured Kerr spectra, a microscopic interpretation is difficult. The probing methods have been extended toward higher photon energies, such as M-edge spectroscopy[12,13] or x-ray magnetic circular dichroism (XMCD).[14] XMCD still detects the magnetization via the spin–orbit coupling but is less affected by state blocking effects as all d states above the Fermi energy are probed and contribute to the magnetic contrast. Recently, the use of high-harmonic light sources in combination with efficient spin polarimeters has led to the measurement of energy- and spin-dependent electron dynamics in ferromagnetic materials.[15,16] In Ref. 16, we report that the electrons close to the Fermi edge show a de-polarization within approximately 60 fs compared to the electrons at $E_F - 2$ eV, which take ≈450 fs for de-polarization.

In this Letter, we compare ultrafast demagnetization measurements performed using the magneto-optical Kerr effect (MOKE) and spin-resolved vacuum ultraviolet photoelectron spectroscopy (SPES) on an ultrathin Fe film on W(110). A similar experiment was conducted in 2011 by Weber *et al.*[17] They compared the demagnetization observed with MOKE and threshold photoemission at a probe photon energy of 5.9 eV. They observe a faster response measured by MOKE compared to the spin resolved photoemission measurements. This is particularly pronounced for higher pump fluences, leading to a demagnetization of 30%. However, due to the low probe photon energy, the cascade of inelastic electrons overlaps with the spectrum of the directly emitted photoelectrons. Therefore, a separation of the spin dynamics at the Fermi edge and at higher binding energies was not possible. In our experiment, we can distinguish the spin dynamics in

the valence band, the states close to the Fermi energy, and the magnetization dynamics measured by MOKE and compare them in the same setup.

A schematic representation of the experimental setup is shown in Fig. 1. The sample is a 20 ML thick iron film grown on a W(110) substrate.[18] It exhibits spontaneous magnetization along the $[\bar{1}10]$ axis that stands perpendicular to the plane formed by the incoming laser beams and the surface normal. The sample is prepared *in situ*, and the pressure inside the vacuum chamber never exceeds 10^{-10} mbar. All laser pulses are initially generated by an amplified Ti:Sa system (Coherent Inc., Legend Elite) operating at a repetition rate of 10 kHz. For photoemission, we use UV laser pulses of a 21 eV photon energy to emit photoelectrons from the sample. The collected photoelectrons are dispersed in energy using a hemispherical energy analyzer (HEA) and subsequently analyzed for their spin polarization with the help of a polarimeter based on spin-polarized low-energy electron diffraction (SPLEED).[19,20] This setup allows us to detect the time-dependent spin dynamics of initially occupied states close to the gamma point along the crystallographic direction ΓN (for more detailed information about this part of the measurement, we refer to the supplementary material). In Fig. 2, we show the measured minority and majority electron distributions from the SPES experiment. The shaded areas show the energy windows used in our experiment. We also indicate the energy window accessible by threshold photoemission experiments.[17]

In the second experimental part, we employ a MOKE detection scheme in transversal geometry (TMOKE) using a 400 nm probe

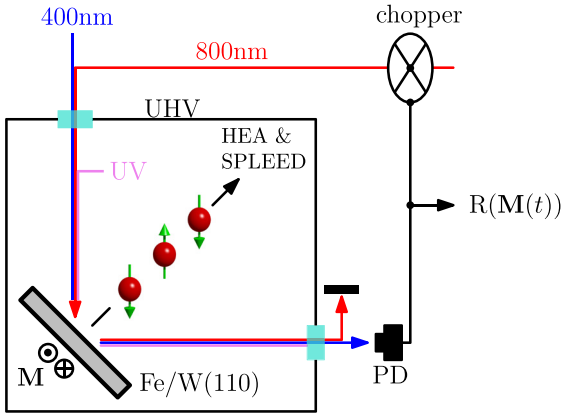

FIG. 1. Ultrafast demagnetization on a Fe/W(110) sample is triggered by a 800 nm pump beam (red). We conduct the same experiment using two different methods: (1) the pump beam is modulated with the help of a chopper. The 400 nm probe beam (blue) probes the transient magnetization via TMOKE. The angles of incidence of the beams are slightly different to avoid spatial overlap in the vacuum windows. A photodiode (PD) picks up the reflected probe beam. Finally, a digital lock-in amplifier detects the pump-induced change in reflectivity. (2) A 21 eV probe beam (violet) from a high-harmonic source (not shown) emits photoelectrons from the sample. An HEA followed by a SPLEED polarimeter analyzes the photoelectrons' kinetic energy and their spin polarization. For this part of the experiment, we do not use the chopper. In both cases, mechanical delay stages (not shown) control the pump-probe delay. All laser pulses originate from the same Ti:Sa amplified laser system. The sample's spontaneous magnetization direction points out of the drawing plane. A coil delivers magnetic field pulses to alter the magnetization as indicated while performing the measurements in remanence. All laser beams are p-polarized.

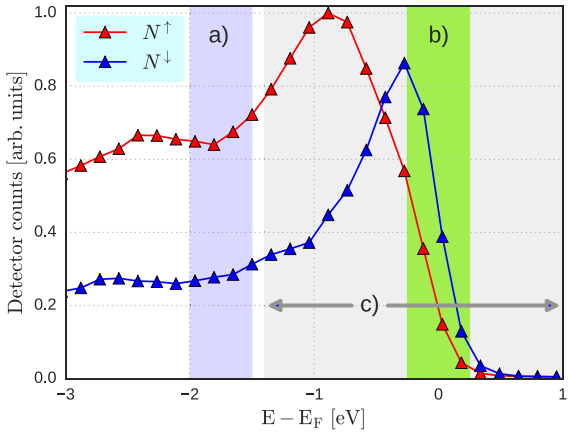

FIG. 2. Measured static photoemission spectra for minority ($N^{\downarrow}$) and majority ($N^{\uparrow}$) electrons. (a) shows the energy range used to determine the dynamics in the valence band. (b) shows the energy range close to the Fermi edge. The gray shaded area (c) depicts the approximate energy range for threshold photoemission at 5.9 eV.[17]

beam, originating from the frequency-doubled fundamental in a beta barium borate crystal. To detect the small pump-induced changes in the reflected intensity, we modulate the pump beam at 891 Hz and record the signal using digital lock-in amplification. The magnetic contribution can be retrieved by taking the difference between opposing magnetization directions $M_{\uparrow}$ and $M_{\downarrow}$. The incident fluence on the sample in the case of the SPES measurement is 6.5 mJ/cm^2. For the TMOKE measurement, we use an incident fluence of 5.6 mJ/cm^2. This corresponds to a depolarization of 25.5% at high binding energy ($E_B = 1.75$ eV, valence band), which is in line with previous studies on similar systems.[17,21] The pulse duration for the 800 nm pulses is measured as 20 fs in front of the vacuum window.

In Ref. 16, we observed the various timescales of depolarization at different energy levels within the probed band structure. Here, we solely record the ultrafast change in spin polarization $\Delta P(t)/P(t \ll 0)$ at two distinct energy levels: in the valence band ($E_F - E = 1.75 \pm 0.25$ eV) and around the Fermi energy ($E - E_F = \pm 0.25$ eV), with a time resolution significantly higher than previously reported. The spin dynamics are compared to the magnetic signal $\Delta M(t) \propto \Delta R(t, M_{\uparrow}) - \Delta R(t, M_{\downarrow})$ recorded by time-resolved TMOKE, as illustrated in the lower panel of Fig. 3. The nonmagnetic part of the pump-induced reflectivity change $\Delta R(t) \propto \Delta R(t, M_{\uparrow}) + \Delta R(t, M_{\downarrow})$, which indicates the electron gas temperature, is scaled to the same magnitude as the actual electron gas temperature T_e. We obtained the latter value by fitting a convolution of the experimental energy resolution and a Fermi-Dirac distribution to the spin-integrated photoemission spectra.[22,23] The point in time when $\Delta R(t)/\Delta R_{max} = \Delta T_e(t)/\Delta T_{e,max} = 0.5$ is chosen as time zero for both measurement schemes. In addition to the electron gas temperature, the time-resolved photoemission spectra provide a measurement of non-thermal electrons. The carriers $\Delta n(t)$ at an energy >0.5 eV above the Fermi energy are shown in the upper panel of Fig. 3 (green). These carriers represent the nonthermal electrons excited by the pump laser pulse.

The lower panel of Fig. 3 shows the depolarization at the Fermi energy level and in the valence band as well as the pump-induced

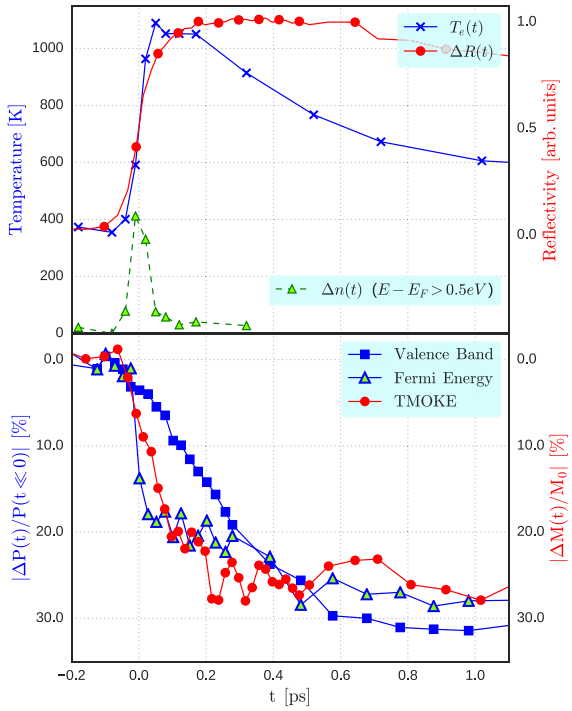

FIG. 3. Data from time-resolved PES measurements are illustrated in blue; data points plotted in red correspond to MOKE measurements. The upper plot shows the electron temperature $T_e(t)$ related to the slope of the spin-integrated photoemission spectrum at the Fermi energy level. In the same plot, we show a scaled version of the transient change in reflectivity measured by TMOKE. The number of nonthermal carriers 0.5 eV above the Fermi energy, in arbitrary units and without a vertical scale, is also illustrated. The lower plot shows the depolarization at the Fermi energy level and in the valence band. The absolute value in the axis labeling on the left-hand side accounts for the opposing signs of polarization at the two energies. The magnetic signal from the TMOKE measurement is scaled with respect to the maximum depolarization in the valence band as determined by a SPES calibration measurement and is referred to as "Demagnetization" $\Delta M(t)/M_0$ (more detailed information can be found in the supplementary material). For better visibility, we applied a Savitzky–Golay filter to the magnetic TMOKE data.

change $\Delta M(t)$ in the magnetic TMOKE signal. For comparison, $\Delta M(t)$ is scaled according to a corresponding measurement of depolarization in the valence band using photoemission (for more information the reader is referred to the supplementary material). The onset of the polarization loss at the Fermi energy coincides with the onset of non-thermal electrons $\Delta n(t)$ (upper panel). The fast decrease is followed by a reduced depolarization rate at longer time delays.

The time resolution between the two experimental methods is not immediately comparable since in both cases pulse autocorrelation has solely been applied to the 800 nm fundamental. Therefore, the probe-pulse duration at the sample cannot be determined unambiguously. However, by analyzing the non-magnetic signals, we can compare the dynamics measured by the different detection methods. Since the ultrafast change of the nonmagnetic MOKE signal is generally seen as proportional to the temperature change of the electron gas, we can exploit this fact to find a point-spread function (PSF), which connects the time resolution of the two experimental methods relatively. Deconvoluting $\Delta R(t)$ with a Lorentzian of 40 fs FWHM, the raising edges of $T_e(t)$ and the resulting values overlap as shown in the upper panel of Fig. 4. We can now use the same point spread function to deconvolve $\Delta M(t)$. However, the data quality of $\Delta M(t)$ does not allow for direct deconvolution of the raw data. Therefore, we apply the deconvolution directly to a standard double exponential fit to the raw TMOKE data [TMOKE (F)]. The result [TMOKE (D)] is presented in the lower panel of Fig. 4. More information about the fitting procedures and the deconvolution algorithm can be found in the corresponding section of the supplementary material.

Based on the results from this analysis, we are now in a position to compare the decay times in the three situations: The polarization at the Fermi energy shows a rapid decrease within $\simeq 50$ fs, possibly limited by our time resolution. In comparison, in the valence band, the depolarization is significantly slower (400 fs). The MOKE measurement shows a demagnetization time of 105 fs, which is similar to the depolarization time at the Fermi edge.

On the femtosecond timescale, the spin polarization is more complex than that in the static case as internal degrees of freedom can be excited within the band structure. In ultrafast magnetism, the

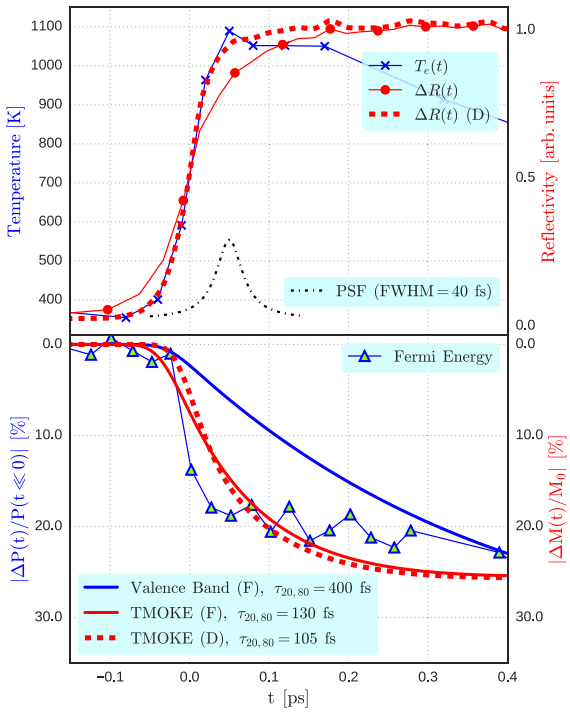

FIG. 4. Data points and lines illustrated in blue correspond to PES measurements, while MOKE related data are shown in red. Data points are presented as markers, while fits (F) and deconvolutions (D) are illustrated using lines. The upper panel shows the deconvoluted change in reflectivity, which is related to the measured $\Delta R(t)$ via a point-spread function (PSF) shown in the same panel without a vertical scale. In the lower panel, we show the fit to the depolarization in the valence band, as well as the fit to the demagnetization measured by TMOKE. The latter is deconvoluted, using the aforementioned point-spread function. The parameter τ indicates the 80%–20% decay time with respect to the minimal value. For more details and aspects about the mentioned analytic methods the reader is referred to the supplementary material. As a comparison to TMOKE (D), the measurement result at the Fermi energy is shown again.

concept of magnetization as the average magnetic moment over a small unit volume is still a valid, well-defined quantity. However, the spin polarization shows different responses to a stimulus depending on which part of the Brillouin zone is probed. From the long history of static experiments in magnetism, we accepted the concept that the MOKE measurement and spin-resolved photoemission detect a quantity directly proportional to the magnetization. Here, we see that this concept is valid ≈300 fs after the pump pulse. However, short after the pump pulse, different measurement techniques start to detect the different aspects of spin dynamics and therefore become much more complementary. This fact makes the different techniques even more valuable in this case than in the quasi-static case.

From Fig. 2, we can see that the threshold photoemission experiment[17] is mainly sensitive to valence electrons as they outnumber the electrons close to the Fermi energy. Therefore, the result from the study by Weber *et al.* is in line with our findings: They also observe faster demagnetization dynamics measured by MOKE compared to photoemission from the valence band. However, the sensitivity of the Mott spin polarimeter does not allow for detecting the spin polarization in an energy and time-resolved manner within the reasonable measurement time. In contrast, our spin-resolved photoelectron spectroscopy experiment provides separate access to spin polarization for different binding energies. In this way, one can detect the responses of the spin system to the pump pulse.[16,24]

As shown by Eich *et al.* for Co and similarly by Gort *et al.* for Fe, the spin dynamics within the valence band are intimately related to ultrafast magnon generation.[16,24] At low binding energy, on the other hand, the microscopic mechanisms driving the depolarization are those in need of empty states near the Fermi energy level: spin-flip scattering processes and spin-polarized transport. The temporal coincidence of Δn_{max} with the fast drop of polarization at the Fermi energy level is an indication for the dominant role of spin-polarized transport and spin flips during laser excitation. In addition, the electrons excited by the pump laser to the Fermi edge originate from the valence band and have majority spin. This also reduces the spin polarization at the Fermi energy within a few femtoseconds.

Still, only a small part of the Brillouin zone is probed by our photoemission setup as already stated in Ref. 16. MOKE spectra; on the other hand, include all possible optical transitions at low binding energy. Momentum microscopes in combination with time-of-flight spectrometers and spin detection have the potential to overcome this limitation because of their ability to map the entire Brillouin zone.[25] However, the spin polarization measured in the valence band is strongly related to the true magnetization, even if we only detect a small part in k space: A change of the spin polarization of fully occupied states requires a modification of the band structure. Two mechanisms causing the band structure change in ferromagnets are discussed: There can be a change of the exchange splitting and the band structure mirroring effect.[16,24] In both cases, this will constitute an overall change of the band structure, which is independent of the location in k space. Therefore, it is likely that the observed dynamics in the valence band represents demagnetization.

In conclusion, we experimentally demonstrate the strong similarity of magneto-optical Kerr measurements with the spin dynamics at the Fermi energy level during ultrafast demagnetization in iron. Most likely, the Kerr measurements are, therefore, sensitive to the states relevant to spin transport and spin flips and are of great importance for future ultrafast spintronic experiments. The states at the Fermi edge are relevant for transport and, therefore, for applications in magnetic sensors. The fact that the spin dynamics at high binding energies differs from the Kerr measurements needs to be considered in future works when parameters extracted from MOKE measurements are used to verify theoretical models. The small acceptance angle of $\pm 4^\circ$ is a limitation of our photoemission experiment. Future photoelectron spectroscopy experiments using the momentum microscope will help to observe the entire Brillouin zone.

See the supplementary material for the details of the experimental techniques, the fitting, and deconvolution methods used in this work.

This work was supported by the Swiss National Science Foundation and ETH Zurich.

REFERENCES

[1]Y. Yang, R. B. Wilson, J. Gorchon, C.-H. Lambert, S. Salahuddin, and J. Bokor, "Ultrafast magnetization reversal by picosecond electrical pulses," Sci. Adv. **3**, e1603117 (2017).
[2]M. H. Kryder, E. C. Gage, T. W. McDaniel, W. A. Challener, R. E. Rottmayer, G. Ju, Y. Hsia, and M. F. Erden, "Heat assisted magnetic recording," Proc. IEEE **96**, 1810–1835 (2008).
[3]E. Beaurepaire, J.-C. Merle, A. Daunois, and J.-Y. Bigot, "Ultrafast spin dynamics in ferromagnetic nickel," Phys. Rev. Lett. **76**, 4250–4253 (1996).
[4]G. Ju, A. Vertikov, A. V. Nurmikko, C. Canady, G. Xiao, R. F. C. Farrow, and A. Cebollada, "Ultrafast nonequilibrium spin dynamics in a ferromagnetic thin film," Phys. Rev. B **57**, R700–R703 (1998).
[5]H. Regensburger, R. Vollmer, and J. Kirschner, "Time-resolved magnetization-induced second-harmonic generation from the Ni(110) surface," Phys. Rev. B **61**, 14716–14722 (2000).
[6]B. Koopmans, M. van Kampen, J. T. Kohlhepp, and W. J. M. de Jonge, "Ultrafast magneto-optics in nickel: Magnetism or optics?," Phys. Rev. Lett. **85**, 844–847 (2000).
[7]L. Guidoni, E. Beaurepaire, and J.-Y. Bigot, "Magneto-optics in the ultrafast regime: Thermalization of spin populations in ferromagnetic films," Phys. Rev. Lett. **89**, 017401 (2002).
[8]T. Kampfrath, R. G. Ulbrich, F. Leuenberger, M. Münzenberg, B. Sass, and W. Felsch, "Ultrafast magneto-optical response of iron thin films," Phys. Rev. B **65**, 104429 (2002).
[9]R. Wilks, R. J. Hicken, M. Ali, B. J. Hickey, J. D. R. Buchanan, A. T. G. Pym, and B. K. Tanner, "Investigation of ultrafast demagnetization and cubic optical nonlinearity of Ni in the polar geometry," J. Appl. Phys. **95**, 7441–7443 (2004).
[10]P. M. Oppeneer and A. Liebsch, "Ultrafast demagnetization in Ni: Theory of magneto-optics for non-equilibrium electron distributions," J. Phys.: Condens. Matter **16**, 5519 (2004).
[11]G. P. Zhang, W. Hubner, G. Lefkidis, Y. Bai, and T. F. George, "Paradigm of the time-resolved magneto-optical Kerr effect for femtosecond magnetism," Nat. Phys. **5**, 499 (2009).
[12]C. La-O-Vorakiat, M. Siemens, M. M. Murnane, H. C. Kapteyn, S. Mathias, M. Aeschlimann, P. Grychtol, R. Adam, C. M. Schneider, J. M. Shaw, H. Nembach, and T. J. Silva, "Ultrafast demagnetization dynamics at the M edges of magnetic elements observed using a tabletop high-harmonic soft x-ray source," Phys. Rev. Lett. **103**, 257402 (2009).
[13]W. You, P. Tengdin, C. Chen, X. Shi, D. Zusin, Y. Zhang, C. Gentry, A. Blonsky, M. Keller, P. M. Oppeneer, H. Kapteyn, Z. Tao, and M. Murnane, "Revealing the nature of the ultrafast magnetic phase transition in Ni by correlating extreme ultraviolet magneto-optic and photoemission spectroscopies," Phys. Rev. Lett. **121**, 077204 (2018).
[14]C. Stamm, T. Kachel, N. Pontius, R. Mitzner, T. Quast, K. Holldack, S. Khan, C. Lupulescu, E. F. Aziz, M. Wietstruk, H. A. Dürr, and W. Eberhardt, "Femtosecond modification of electron localization and transfer of angular momentum in nickel," Nat. Mater. **6**, 740 (2007).

[15]S. Eich, A. Stange, A. Carr, J. Urbancic, T. Popmintchev, M. Wiesenmayer, K. Jansen, A. Ruffing, S. Jakobs, T. Rohwer, S. Hellmann, C. Chen, P. Matyba, L. Kipp, K. Rossnagel, M. Bauer, M. Murnane, H. Kapteyn, S. Mathias, and M. Aeschlimann, "Time- and angle-resolved photoemission spectroscopy with optimized high-harmonic pulses using frequency-doubled Ti: Sapphire lasers," J. Electron Spectrosc. Relat. Phenom. **195**, 231–236 (2014).
[16]R. Gort, K. Bühlmann, S. Däster, G. Salvatella, N. Hartmann, Y. Zemp, S. Holenstein, C. Stieger, A. Fognini, T. U. Michlmayr, T. Bähler, A. Vaterlaus, and Y. Acremann, "Early stages of ultrafast spin dynamics in a 3d ferromagnet," Phys. Rev. Lett. **121**, 087206 (2018).
[17]A. Weber, F. Pressacco, S. Günther, E. Mancini, P. M. Oppeneer, and C. H. Back, "Ultrafast demagnetization dynamics of thin Fe/W(110) films: Comparison of time- and spin-resolved photoemission with time-resolved magneto-optic experiments," Phys. Rev. B **84**, 132412 (2011).
[18]S. Miesch, A. Fognini, Y. Acremann, A. Vaterlaus, and T. U. Michlmayr, "Fe on W(110), a stable magnetic reference system," J. Appl. Phys. **109**, 013905 (2011).
[19]C. Tusche, M. Ellguth, A. A. Ünal, C.-T. Chiang, A. Winkelmann, A. Krasyuk, M. Hahn, G. Schönhense, and J. Kirschner, "Spin resolved photoelectron microscopy using a two-dimensional spin-polarizing electron mirror," Appl. Phys. Lett. **99**, 032505 (2011).
[20]M. Kolbe, P. Lushchyk, B. Petereit, H. J. Elmers, G. Schönhense, A. Oelsner, C. Tusche, and J. Kirschner, "Highly efficient multichannel spin-polarization detection," Phys. Rev. Lett. **107**, 207601 (2011).
[21]E. Carpene, E. Mancini, C. Dallera, M. Brenna, E. Puppin, and S. D. Silvestri, "Dynamics of electron-magnon interaction and ultrafast demagnetization in thin iron films," Phys. Rev. B **78**, 174422 (2008).
[22]T. Greber, T. J. Kreutz, and J. Osterwalder, "Photoemission above the fermi level: The top of the minority d band in nickel," Phys. Rev. Lett. **79**, 4465–4468 (1997).
[23]J. Kröger, T. Greber, T. Kreutz, and J. Osterwalder, "The photoemission fermi edge as a sample thermometer?," J. Electron Spectrosc. Relat. Phenom. **113**, 241–251 (2001).
[24]S. Eich, M. Plötzing, M. Rollinger, S. Emmerich, R. Adam, C. Chen, H. C. Kapteyn, M. M. Murnane, L. Plucinski, D. Steil, B. Stadtmüller, M. Cinchetti, M. Aeschlimann, C. M. Schneider, and S. Mathias, "Band structure evolution during the ultrafast ferromagnetic-paramagnetic phase transition in cobalt," Sci. Adv. **3**, e1602094 (2017).
[25]D. Kutnyakhov, S. Chernov, K. Medjanik, R. Wallauer, C. Tusche, M. Ellguth, S. A. Nepijko, M. Krivenkov, J. Braun, S. Borek, J. Minár, H. Ebert, H. J. Elmers, and G. Schönhense, "Spin texture of time-reversal symmetry invariant surface states on W(110)," Sci. Rep. **6**, 29394 (2016).